



X-ray measurements of highly charged Ar ions passing through a Ni microcapillary: Coincidence of L X-rays and final charge states

Y. Kanai ^{a,*}, Y. Nakai ^a, Y. Iwai ^a, T. Ikeda ^a, M. Hoshino ^a, K. Nishio ^b,
H. Masuda ^b, Y. Yamazaki ^{a,c}

^a Atomic Physics Laboratory, RIKEN, Wako, Saitama 351-0198, Japan

^b Department of Applied Chemistry, Tokyo Metropolitan University, Hachioji, Tokyo 192-0397, Japan

^c Institute of Physics, Graduate School of Arts and Sciences, The University of Tokyo, Meguro, Tokyo 153-8902, Japan

Available online 27 April 2005

Abstract

We have made coincidence measurements between L X-rays and final charge states of highly-charged Ar ions passing through a Ni microcapillary thin foil to study the formation and relaxation processes of hollow atoms. By using N^{6+} projectile ions which have single K-shell hole, Ninomiya et al. [Phys. Rev. Lett. 78 (1997) 4557] showed the existence of long lived excited states formed by multiple electron transfer from a Ni microcapillary thin foil. To further study the formation and relaxation dynamics, such experiments were extended to Ar ions with multiple L-shell holes. The yields of L X-rays from Ar ions, which have one stabilized-electron, decrease faster than those from ions with multiple stabilized-electrons, when the projectiles have multiple inner shell holes.

© 2005 Elsevier Ltd. All rights reserved.

PACS: 34.50.Dy

Keywords: Hollow atoms; Microcapillary; Slow highly charged ions

1. Introduction

When a slow highly charged ion (HCI) approaches a metal surface, the ion is accelerated toward the surface due to its image charge and then the ion resonantly captures target electrons into its excited states. According to the classical

* Corresponding author. Tel.: +81 48 467 9486; fax: +81 48 462 4644.

E-mail address: kanai@rarfaxp.riken.go.jp (Y. Kanai).

over-barrier (COB) model [1–3], the resonant charge transfer starts at a distance $d_c \sim (2q_i)^{1/2}/W$, and the first electrons are transferred to states with principal quantum number $n_c \sim q_i/[2W(1 + (q_i - 0.5)/(8q_i)^{1/2})]^{1/2}$ of the incident ion, where q_i is the charge state of the ion and W is the work function of the solid. Note that the physical quantities are in atomic units unless otherwise noted. Such an atom (ion) with multiply excited electrons and inner shell holes is called a “hollow atom (ion)”. The formation and relaxation dynamics of hollow atoms have been studied intensively in recent years [1–10]. By using conventional flat-surface targets, it is difficult to observe the structure and dynamical features of hollow atom above the surface, because its intrinsic lifetime could be longer than the time interval (i.e. $\sim 10^{-13}$ s) between the hollow atom formation above the surface and its arrival at the surface. To overcome the difficulty, we have employed microcapillary targets [11,12] to produce hollow atoms (ions) and extract them in vacuum. The microcapillary used in our experiments was ~ 1 mm² in size with a thickness of $\sim \mu\text{m}$ and had a multitude of straight holes of ~ 100 nm in diameter. When HCIs impinge on the microcapillary target parallel to the capillary axis, a part of the hollow atoms (ions) formed in the capillary can pass through it before hitting the capillary wall and free hollow ions are extracted in vacuum [13–22]. By using N⁶⁺ projectile ions with single K-shell hole and a Ni microcapillary thin foil, Ninomiya et al. [14] showed the existence of long lived excited states as an evidence of free hollow ions formed by multiple electron transfer. These states have multiple electrons in the L shell and/or in higher shells keeping a K-shell hole, and such K-shell hole has a extremely long lifetime of the order nanosecond to be filled. Morishita et al. [20] verified that the first transfer of an electron from a metal surface takes place near n_c with a narrow distribution width of $\Delta n \sim 2$, the average number of which agrees quite well with the prediction of the COB model. Regarding the decay processes of hollow atoms, on the other hand, our knowledge is quite limited. To obtain such information, we have measured L X-rays in coincidence with the final charge states for Ar^{q_f+} ions having multiple inner shell holes as projectiles.

2. Experiments

The experiments were performed with a Ni microcapillary thin target [11,12] and highly charged Ar ions from a 14.5 GHz caprice ECR ion source at RIKEN [23]. A schematic drawing of our experimental setup is shown in Fig. 1. Ar^{q_i+} ions ($q_i = 14, 13, 11, 9$) extracted from the ion source with the energy of 2.8 keV/amu were collimated and impinged on the Ni microcapillary foil in parallel to the capillary axis. Downstream of the target, the Si(Li) detector was placed at right angle to the beam axis. The distance between the Si(Li) crystal and the beam axis was 36 mm. The diameter of the entrance aperture of the Si(Li) detector was 6 mm and the distance between the entrance aperture and the Si(Li) crystal was 16 mm. The effective area of the Si(Li) crystal was about 30 mm². The shield which was movable along the beam direction was located between the target and the Si(Li) detector and was used to define the part of the beam path from which the emitted X-rays were detected. The distance from the shield and the beam axis was 5.2 mm. Roughly speaking, when the edge of the shield is at z mm from the target exit surface, the detector can capture X-rays emitted at time $14 \text{ ns} > t_d \geq z/v$ after the passage of the target, where v is the projectile velocity and $v = 0.74$ mm/ns for the present case. The X-rays emitted after 14 ns were cut by the entrance aperture of the Si(Li) detector. After stabilization of the captured electrons, Ar ions were selected with their charge states by the electrostatic charge state analyzer and detected by the channel electron multiplier (CEM). The charge state analyzer was set at ~ 20 cm downstream from the target. The difference between the initial q_i and final q_f charge state of Ar ions gives the number of the stabilized electrons after the decay processes; $N_s = q_i - q_f$.

The L X-rays emitted from the Ar ions after the target were measured in coincidence with the final charge state q_f . The lifetime of the L-shell hole of the transmitted ions was determined through the dependence of the X-ray yield on the shield position, which is given by

$$\eta(z, q_f) = \int_{z/v}^T \zeta(z'/v, q_f) C(z') dz'/v \quad (1)$$

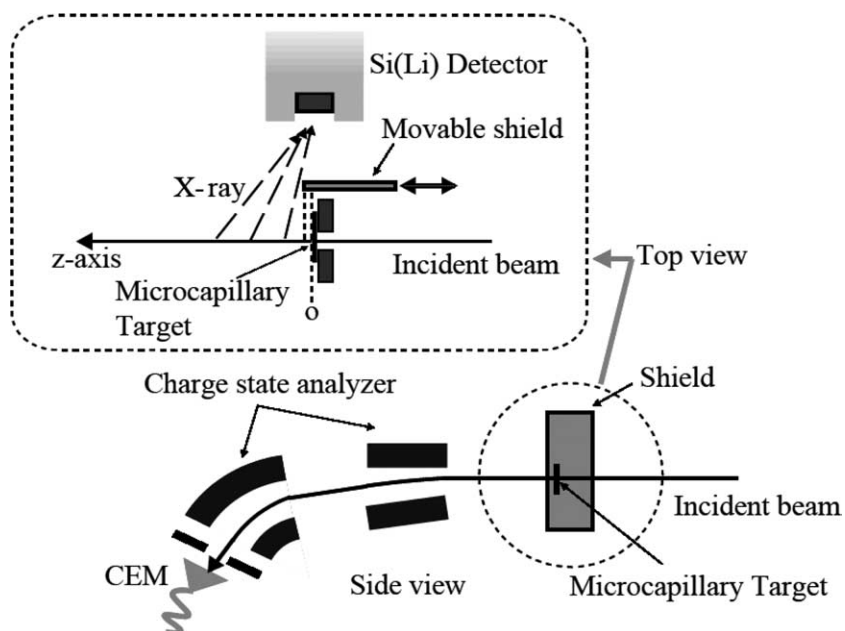


Fig. 1. Schematic drawing of experimental setup.

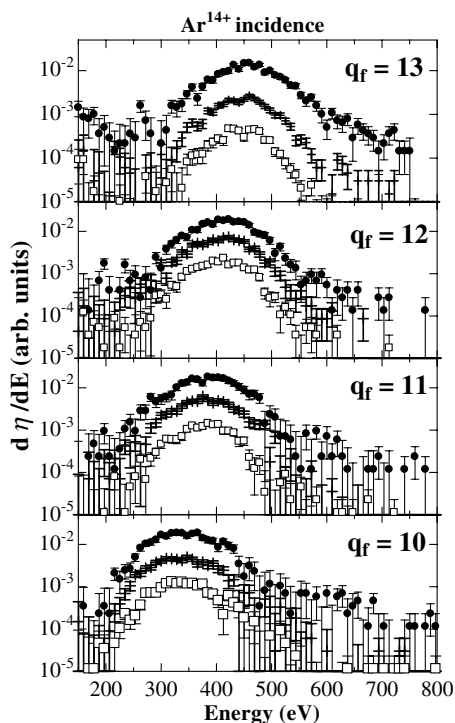
where $\zeta(z'/v, q_f)$ is the intensity of X-rays emitted at z' from the target from the ions with their final charge states q_f , $C(z')$ is the geometrical factor for the detector's solid angle at z' , and T is the maximum observable delay time where $T = 14$ ns in this experiment. In this paper, we use $C(z')$ as constant to simplify the analysis. Detailed discussion of the detection efficiency will be published in somewhere [24].

3. Results and discussion

3.1. Peak positions of X-ray spectra

Typical coincidence X-ray spectra $d\eta(z, q_f)/dE$ at $z = 0, 2,$ and 4 mm for Ar^{q_i+} ($q_i = 14, 13, 11, 9$) are shown in Figs. 2–5, which shows;

- (i) the peak energy of the coincidence X-ray spectrum shifts to a lower energy with decreasing final charge states q_f , i.e. with increasing the number of stabilized electrons N_s , and does not depend on the shield position z , i.e. the delay time t_d ,

Fig. 2. Delay time dependence of L X-ray spectra in coincident with final charge states Ar^{q_f+} , $q_f = 13, 12, 11, 10$ for Ar^{14+} projectile for $z = 0$ mm (\bullet), 2 mm ($+$), and 4 mm (\square).

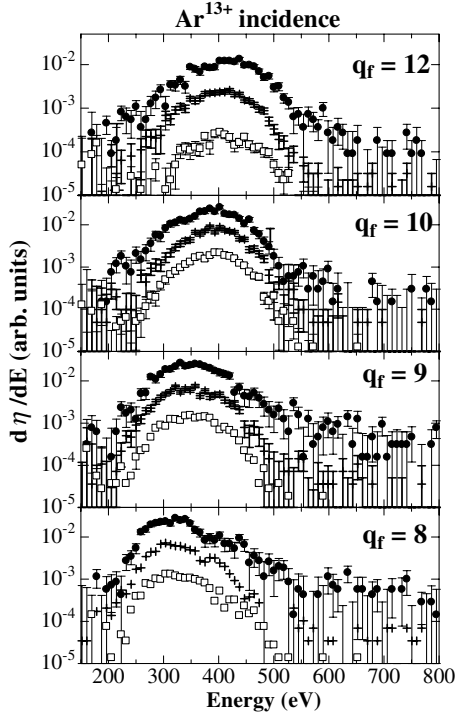


Fig. 3. Delay time dependence of L X-ray spectra in coincident with final charge states Ar^{q_f+} , $q_f = 12, 11, 10, 9$ for Ar^{13+} projectile for $z = 0$ mm (\bullet), 2 mm ($+$), and 4 mm (\square).

(ii) the shape of the X-ray spectrum dose not depend on the shield position z .

These observations indicate that the core charge states of Ar ions at the moment of L X-ray emission depend only on the final charge state q_f and do not depend on the delay time after the target.

Coincidence X-ray spectra for $z = 2$ mm ($t_d \geq 2.7$ ns) are compared in Fig. 6 for different incident charge states q_i . The peak energies of X-rays for $q_i = 14, q_f = 12, 11, 10$ are almost same as those for $q_i = 13, q_f = 12, 11, 10$, respectively, that is, the peak energies of coincidence X-ray spectra seem to depend on the final charge state q_f but not depend on the initial charge states q_i .

We interpret these features as follows: Among the stabilized N_s electrons, $(N_s - 1)$ electrons rapidly (\ll ns) filled the L-shell holes by a cascade of Auger processes [1,2,25,26], and then the last N_s th electron slowly filled the L-shell hole by a

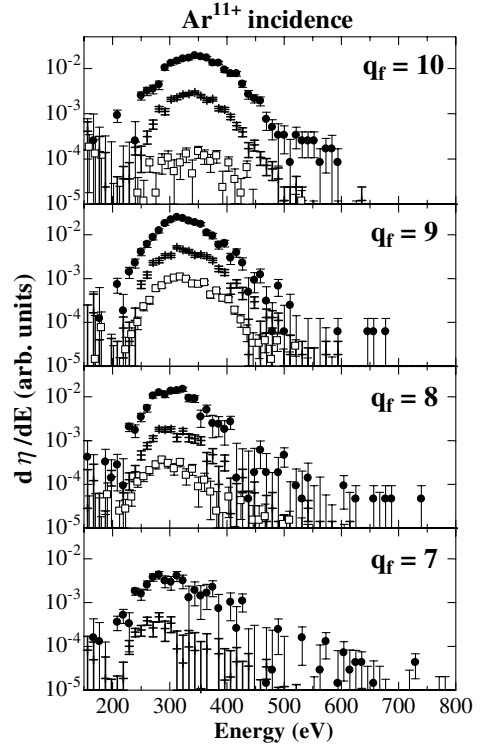


Fig. 4. Delay time dependence of L X-ray spectra in coincident with final charge states Ar^{q_f+} , $q_f = 10, 9, 8, 7$ for Ar^{11+} projectile for $z = 0$ mm (\bullet), 2 mm ($+$), and 4 mm (\square).

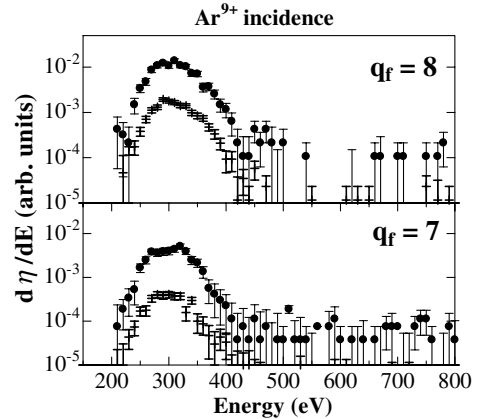


Fig. 5. Delay time dependence of L X-ray spectra in coincident with final charge states Ar^{q_f+} , $q_f = 8, 7$ for Ar^{9+} projectile for $z = 0$ mm (\bullet) and 2 mm ($+$).

radiative cascade ending with emitting L X-rays, where the core charge state is “ $(q_i - N_s + 1)$ ”. Of

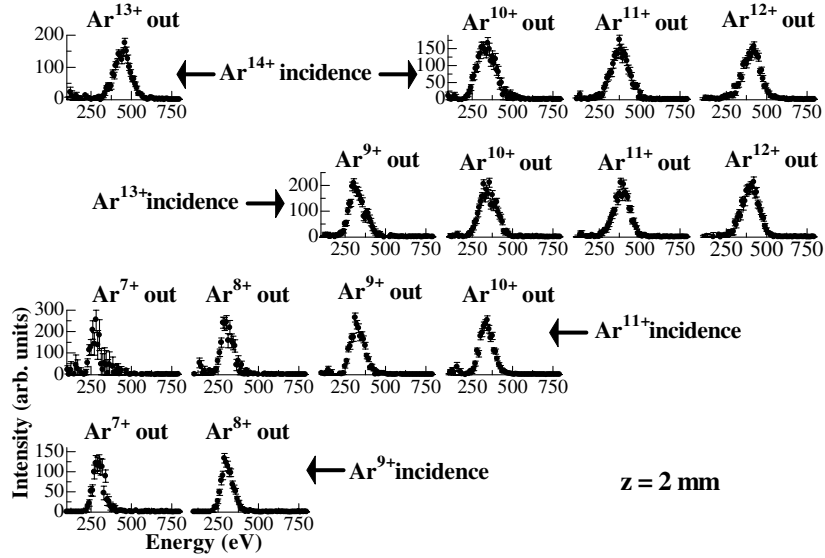


Fig. 6. X-ray spectra for $z = 2$ mm ($t_d = 2.7$ ns). To compare X-ray spectrum for different initial charge states q_i , peak heights are not normalized.

course, this is not true for the case of $N_s > N_0$, where N_0 is the number of the initial L-shell holes. In this case the core charge state is always “9+” at the moment of the L X-ray emission.

3.2. Delayed X-ray yields

The integrated delayed X-ray yields $\eta(z, q_f)$ normalized per Ar^{q_f} ion with q_f for $q_i = 14, 13, 11, 9$ are shown in Fig. 7. The corresponding time range is 0–14 ns and the time resolution is ~ 1 ns [24]. Fig. 6 shows the following features:

- (1) the integrated delayed X-ray yields show the long decay rate (\sim ns).
- (2) the integrated delayed X-ray yields for single-electron stabilized ions ($N_s = 1$) decrease more rapidly than those for multi-electron stabilized ions ($N_s \geq 2$), except for $q_i = 9$.
- (3) the integrated X-ray yields for $z = 0$ mm are almost same, when the ions have multiple L-shell holes at the moment of the X-ray emission.

Here, we mainly focus on the feature (2). According to the assumption in the previous section, $(N_s - 1)$ of L-shell holes are filled by a cas-

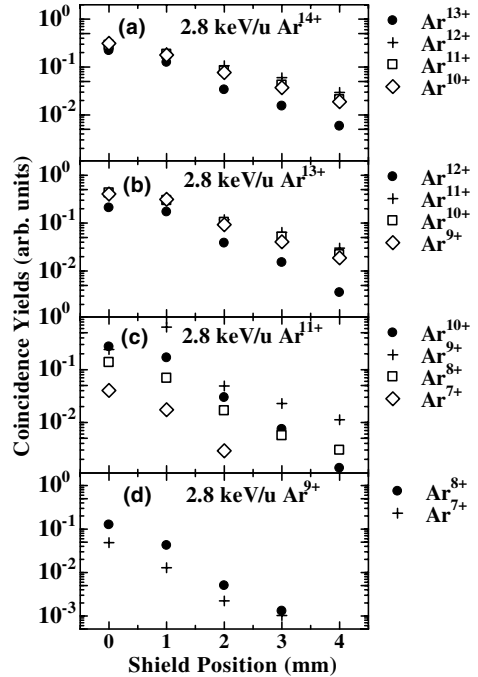


Fig. 7. The integrated delayed X-ray yields normalized per one Ar^{q_f} ion as a function of delay time. (a) $q_f = 13$ (\circ), 12 ($+$), 11 (\square), and 10 (\diamond) for Ar^{14+} projectile, (b) $q_f = 12$ (\circ), 11 ($+$), 10 (\square), and 9 (\diamond) for Ar^{13+} projectile, (c) $q_f = 10$ (\circ), 9 ($+$), 8 (\square), and 7 (\diamond) for Ar^{11+} projectile, (d) $q_f = 8$ (\circ), and 7 ($+$) for Ar^{9+} projectile.

cade of Auger processes rapidly and then the N_s th hole is filled by emitting L X-rays. So, the z -dependence of the integrated delayed X-ray yields $\eta(z, q_f)$ primarily reflects the filling process of the N_s th L-shell hole, where $1 \leq N_s \leq N_0$. Many L X-ray transitions from the M-shell are reported [27] around the peak-energy region of each spectrum shown in Figs. 2–5. So, main parts of the observed L X-rays seem to be emitted by the transition from the M shell to the L shell. Let's assume that the observed decay time τ_o of X-ray intensity is given by

$$\tau_o = \tau_A + \tau_d + \tau_{\text{LX-rays}} \quad (2)$$

where τ_A is the decay time for a cascade of Auger processes to fill the $(N_s - 1)$ holes leaving one electron in an excited state (n_0, l_0) , τ_d is the decay time for a cascade of radiative transitions from the (n_0, l_0) state to $n = 3$ states, $\tau_{\text{LX-rays}}$ is the decay time of N_s th L-shell hole filled by the M-shell electron by emitting L X-rays. In general, Auger cascade processes of multiply excited states are rapid. So, τ_o may be reduced as

$$\tau_o \sim \tau_d + \tau_{\text{LX-rays}}. \quad (3)$$

It is difficult to explain the difference between the observed lifetime for $N_s = 1$ and that for $N_s \geq 2$, by the difference of $\tau_{\text{LX-rays}}$. Because,

there is no reason that the $\tau_{\text{LX-rays}}$ for $N_s = 1$ must be always shorter than that for $N_s \geq 2$. Therefore, we consider that τ_d is different between the $N_s = 1$ and $N_s \geq 2$. cases. As mentioned before, according to the COB model [1–3], electrons are resonantly transferred from the conduction band of metal into the excited states (n_c, l) of Ar ion. Using the value of 0.191 a.u. for the work function W of Ni metal, $n_c = 10.3, 12.2, 14.1,$ and 15.0 are obtained for $q_i = 9, 11, 13,$ and $14,$ respectively. Here, let's assume many electrons are transferred into excited states of $n \sim n_c$, to simplify the discussion. The excited electrons decay by a cascade of Auger processes and fill the $(N_s - 1)$ L-shell holes, leaving one electron in an excited state (n_0, l_0) . If the electron in the excited state (n_0, l_0) is a spectator of the Auger processes, n_0 is $\sim n_c$, and if the electron in the excited state (n_0, l_0) is a participator of the Auger processes, n_0 must be smaller than n_c . If multiple electrons are transferred at first, the last electron in the excited state (n_0, l_0) for $N_s = 1$ should be the participator of Auger processes, and that for $N_s \geq 2$ can be the spectator, as shown in Fig. 8. The decay time for a cascade of radiative transitions from the excited state (n_0, l_0) to the M-shell for $N_s = 1$ can be shorter than that for $N_s \geq 2$. If the excited state (n_0, l_0) has a small angular momentum, such as s, p, and d, the excited

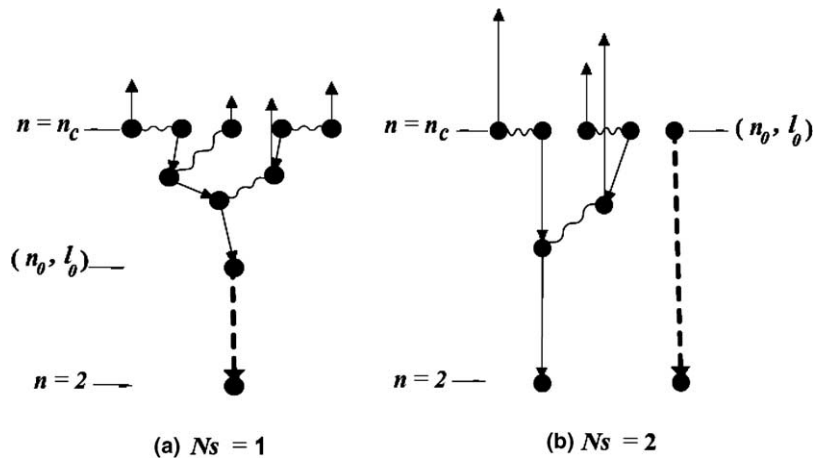


Fig. 8. Schematic diagram for a cascade of Auger processes followed by a radiative cascade. Solid circles (●) indicate electrons. Each wave line connects a pair of electrons participated in single Auger processes. Broken allows indicate a radiative cascade. Five electrons in the initial excited states ($n = n_c$) decay by a cascade of Auger processes leaving one electron in the excited state (n_0, l_0) . (a) $N_s = 1$ case. n_0 should be smaller than n_c . (b) $N_s = 2$ case. In the extreme case, n_0 can be n_c .

electron rapidly decays into the L-shell hole by emitting X-rays. So, our observed \sim ns lifetime should be related to the higher angular momentum excited states (n_0, l_0) , $l_0 \gg 1$.

Here, we have to mention that the above discussion is true when the single electron stabilized ($N_s = 1$) ions are mainly produced by the multiple electron transfer followed by a cascade of Auger processes. Although it is supported by the recent simulations [3,25], it has not been verified by the experiments. If the single electron stabilized ($N_s = 1$) ions are mainly produced by the single electron transfer processes, there should be other mechanism to cause that the τ_d for $N_s = 1$ is shorter than that for $N_s \geq 2$.

4. Summary

We have made coincidence measurements between L X-rays and final charge states of Ar ions transmitted through a Ni microcapillary. Observed decay profile of the L X-ray yields strongly depend on the number N_s of the stabilized electrons, when the initial Ar ions have multiple L-shell holes: The observed intensity of the L X-rays decreases faster for $N_s = 1$ than those for $N_s \geq 2$. We describe the experimental results by assuming a decay process where a cascade of fast Auger processes fills the $(N_s - 1)$ L-shell holes and then slower radiative cascades of the last-remained excited electron fills the L-shell hole by emission of an L X-ray.

Acknowledgement

We thank Dr. T. Kambara for helpful comments on the manuscript. This work is partly supported by a Grand-in-Aid for Scientific Research from Japan Society for the Promotion of Science.

References

[1] J. Burgdörfer, P. Lerner, F.W. Meyer, Phys. Rev. A 44 (1991) 5674.

- [2] J. Burgdörfer, in: C.D. Lin (Ed.), Review of Fundamental Processes and Applications of Atoms and Ions, World Scientific, Singapore, 1993, p. 517.
- [3] K. Tökési, L. Wirtz, C. Lemell, J. Burgdörfer, Phys. Rev. A 64 (2001) 042902.
- [4] J.P. Briand, L. de Billy, P. Charles, S. Essabaa, Phys. Rev. Lett. 65 (1990) 159.
- [5] H.J. Andrä, A. Simionovici, T. Lamy, A. Brenac, G. Lambole, J.J. Bonnet, A. Fleury, M. Bonnefoy, M. Chassevent, S. Andriamonje, A. Pesnell, Z. Phys. D 21 (1991) S135.
- [6] H. Winter, Europhys. Lett. 18 (1992) 207.
- [7] F. Aumayr, H. Kurz, D. Schneider, M.A. Briere, J.W. McDonald, C.E. Cunningham, H.P. Winter, Phys. Rev. Lett. 71 (1993) 1943.
- [8] F.W. Meyer, S.H. Overbury, C.C. Havener, P.A. Zeijlmans van Emmichoven, D.M. Zehner, Phys. Rev. Lett. 67 (1991) 723.
- [9] J. Das, R. Morgenstern, Phys. Rev. A 47 (1993) R755.
- [10] R. Köhrbrück, M. Grether, A. Spieler, N. Stolterfoht, Phys. Rev. A 50 (1994) 1429.
- [11] H. Masuda, K. Fukuda, Science 268 (1995) 1466.
- [12] H. Masuda, M. Satoh, Jpn. J. Appl. Phys. 35 (1996) L126.
- [13] Y. Yamazaki, S. Ninomiya, F. Koike, H. Masuda, T. Azuma, K. Komaki, K. Kuroki, M. Sekiguchi, J. Phys. Soc. Jpn. 65 (1996) 1199.
- [14] S. Ninomiya, Y. Yamazaki, F. Koike, H. Masuda, T. Azuma, K. Komaki, K. Kuroki, M. Sekiguchi, Phys. Rev. Lett. 78 (1997) 4557.
- [15] S. Ninomiya, Y. Yamazaki, T. Azuma, K. Komaki, F. Koike, H. Masuda, K. Kuroki, M. Sekiguchi, Phys. Scripta T 73 (1997) 316.
- [16] Y. Morishita, S. Ninomiya, Y. Yamazaki, K. Komaki, K. Kuroki, H. Masuda, M. Sekiguchi, Phys. Scripta T 80 (1999) 212.
- [17] Y. Yamazaki, Phys. Scripta T 73 (1997) 293.
- [18] Y. Yamazaki, Int. J. Mass Spectro. 192 (1999) 437.
- [19] Y. Kanai, K. Ando, T. Azuma, R. Hutton, K. Ishii, T. Ikeda, Y. Iwai, K. Komaki, K. Kuroki, H. Masuda, Y. Morishita, K. Nishio, H. Oyama, M. Sekiguchi, Y. Yamazaki, Nucl. Instr. and Meth. B 182 (2001) 174.
- [20] Y. Morishita, R. Hutton, H.A. Torii, K. Komaki, T. Brage, K. Ando, K. Ishii, Y. Kanai, H. Masuda, M. Sekiguchi, F.B. Rosmej, Y. Yamazaki, Phys. Rev. A 70 (2004) 012902.
- [21] Y. Iwai, D. Murakoshi, Y. Kanai, H. Oyama, K. Ando, H. Masuda, K. Nishio, M. Nakao, T. Tamamura, K. Komaki, Y. Yamazaki, Nucl. Instr. and Meth. B 193 (2002) 504.
- [22] Y. Iwai, Y. Kanai, Y. Nakai, T. Ikeda, H. Oyama, K. Ando, H. Masuda, K. Nishio, M. Nakao, H.A. Torii, K. Komaki, Y. Yamazaki, Nucl. Instr. and Meth. B 205 (2003) 762.
- [23] Y. Kanai, D. Dumitriu, Y. Iwai, T. Kambara, T.M. Kojima, A. Mohri, Y. Morishita, Y. Nakai, H. Oyama, N. Oshima, Y. Yamazaki, Phys. Scripta T 92 (2001) 467.

- [24] Y. Iwai, Y. Kanai, Y. Nakai, T. Ikeda, M. Hoshino, H. Oyama, K. Ando, H. Masuda, K. Nishio, H.A. Torii, K. Komaki, Y. Yamazaki, *Nucl. Instr. and Meth. B*, in press, doi:10.1016/j.nimb.2005.03.226.
- [25] K. Tórkési, private communications.
- [26] S. Martin, L. Chen, R. Brédy, J. Bernard, A. Salmoun, B. Wei, *Phys. Rev. A* 69 (2004) 043202.
- [27] R.L. Kelly, *J. Phys. Chem. Ref. Data* 16 (Suppl. 1) (1987).